

Automated Extended Volume Imaging of Tissue using Confocal and Optical Microscopy

G.B. Sands, D.A. Gerneke, B.H. Smaill and I.J. Le Grice
Bioengineering Institute, The University of Auckland, Auckland, New Zealand
email: g.sands@auckland.ac.nz

Abstract—Conventional histologic techniques cannot readily be used for 3D reconstruction of large tissue volumes. We have developed an imaging rig which supports both confocal and light microscopy, and utilizes a surface imaging approach to serially image embedded tissue blocks while maintaining alignment and registration of the image series.

I. INTRODUCTION

A variety of techniques are commonly used for imaging 3D tissue structure. Both MRI and CT (including micro-CT) are used where contrast is amenable for resolutions between 10 μm and 10 mm. With conventional microscopy, micron-scale resolution is achieved by imaging thin sections. 3D tissue structures have been reconstructed at this resolution by serial sectioning and imaging. However, this approach is prone to alignment errors. These problems are resolved using confocal microscopy, but tissue depths that can be imaged are limited, nonetheless.

We have constructed a system which enables accurately registered microscopic images to be acquired throughout relatively large tissue volumes (up to tens of millimeters in dimension). Serial images are acquired from the upper surface of embedded specimens mounted on a 3-axis translation stage. Surface tissue is sequentially removed to image through the volume.

II. METHODS

A. Equipment

The imaging rig [1] is shown in Fig. 1. The individual components identified in this figure are mounted on an optical table (Newport Corporation, Irvine, CA). The 3-axis translation stage (Aerotech, Pittsburgh, PA) uses linear motors to move the sample between imaging and tissue processing equipment, while maintaining registration of better than 300 nm. The Leica TCS 4D confocal microscope (Leica Microsystems AG, Wetzlar, Germany) was modified by removing the base and Z-scan stage, and rigidly mounted on the optical table. An Omnichrome® krypton-argon laser (Melles Griot, Carlsbad, CA) routed through a 4-band acousto-optical tunable filter illuminated the sample through the microscope. The Canon 1D MarkII digital camera (Canon Inc., Tokyo, Japan) was equipped with the MP-E 65 mm macro lens with 1-5 \times zoom, and mounted above the stage. Tissue removal

This work was supported by The Wellcome Trust and the Health Research Council of New Zealand.

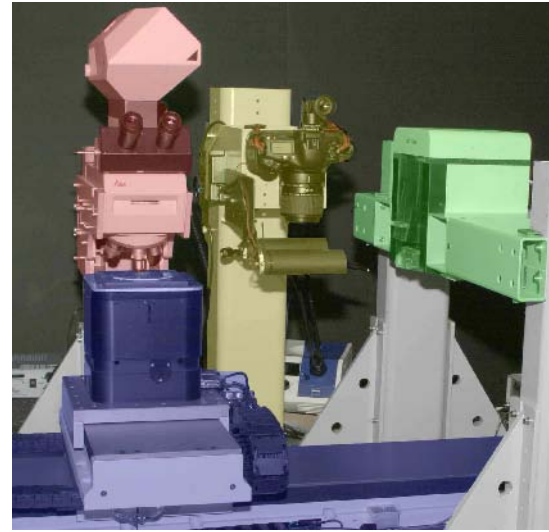


Fig. 1. A three-axis translation stage (blue) moves the sample between the confocal microscope (red) or digital camera (yellow) and the tissue processing ultramill (green).

was performed using a Leica SP2600 ultramill equipped with a two-bladed diamond-tipped flywheel cutter.

Custom software was written for image acquisition and processing using LabVIEW™ (National Instruments, Austin, TX), and volume rendering of 3D images was performed using Voxx (<http://www.nephrology.iupui.edu/imaging/voxx/>) [2].

B. Tissue Processing

Four tissue samples are used to illustrate the image acquisition capabilities of this system. Cardiac ventricle and cortical brain tissue were imaged using the confocal microscope, while the digital camera was used to image cochlea and atrial tissue. All tissue processing was approved by the University of Auckland Animal Ethics Committee.

1) *Cardiac ventricle*: Established protocols [3] were used to arrest and fix a Wistar-Kyoto rat heart in Bouin's fixative, followed by perfusion with picosirius red (PSR) which binds preferentially to collagen. A transmural section (2 mm \times 2 mm \times 4 mm) was cut from the heart, dehydrated in a graded series of ethanols followed by propylene oxide, and embedded in Procure 812 resin (ProSciTech, Qld, Australia) and polymerized for 12 h at 60 °C.

The embedded sample was epoxied to an aluminium sample plate, screwed to the Z-stage, and milled until the tissue

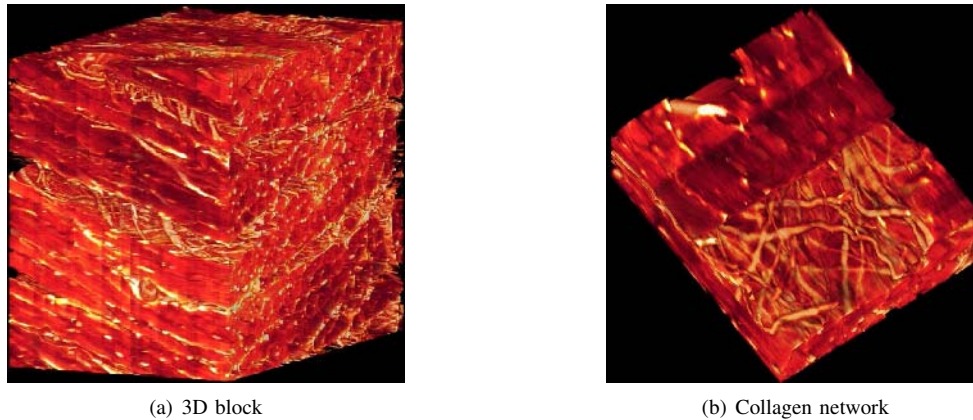


Fig. 2. Cardiac ventricular tissue stained with PSR. (a) Block dimensions are $200\ \mu\text{m} \times 200\ \mu\text{m} \times 200\ \mu\text{m}$. Collagen is visible surrounding cells, and strands run between cells. (b) A closeup view reveals the criss-cross collagen network that binds fibers into layers.

was exposed in the resin. Images were acquired with the confocal microscope using a rhodamine-based filter setting and a $20\times/0.7$ NA water-immersion lens with $2.45\times$ zoom. The image field was $205\ \mu\text{m} \times 205\ \mu\text{m}$ with a pixel resolution of $0.4\ \mu\text{m}$. A serial imaging procedure was used to acquire 3D image information [1]. The sample was imaged at 51 image planes over $20\ \mu\text{m}$ ($0.4\ \mu\text{m}$ spacing) with a regular grid of 6×6 images (50% overlapped) on each plane. $18\ \mu\text{m}$ of the block was then milled, and the image process repeated for 21 such image-mill cycles, totaling 1071 image planes and a total image depth of $428\ \mu\text{m}$.

2) *Brain cortex*: Brain tissue was excised from rat cortex and immersion fixed using 1% paraformaldehyde, then labeled for glial fibrillary acidic protein (GFAP) using a directly linked Cy3 fluorochrome (Sigma-Aldrich, St. Louis, MO) and embedded in a water-soluble melamine resin (Nanoplast®, Agar Scientific, Stansted, UK). Details of the milling procedure are given elsewhere [4].

The resin-embedded sample was mounted on the stage, and milled to expose the tissue surface. Images were acquired with the confocal microscope again using a rhodamine-based filter setting and $20\times/0.7$ NA water-immersion objective. $2\times$ line averaging was employed with a $1.95\times$ zoom. The image field was $256\ \mu\text{m} \times 256\ \mu\text{m}$ with a pixel resolution of $0.5\ \mu\text{m}$. An overlapping grid of 3×3 images was acquired on 60 planes over $30\ \mu\text{m}$ ($0.5\ \mu\text{m}$ spacing). $25\ \mu\text{m}$ of tissue was then milled, and this process repeated for 15 such image-mill cycles. A total of 900 image planes were acquired over a total depth of $380\ \mu\text{m}$.

3) *Cardiac atria*: The right atrial appendage was dissected from pig hearts perfusion fixed with 3% formalin. The tissue ($60\ \text{mm} \times 40\ \text{mm} \times 9\ \text{mm}$) was flattened, dehydrated in a graded series of ethanols followed by Xylene, before embedding in paraffin wax (Kendal Paraplast, $56\ ^\circ\text{C}$ melting point, Kendall Healthcare, Mansfield, MA, USA).

The wax-embedded sample was mounted on the stage. Following each mill step, the wax surface was etched for 10s using 25% xylol in 100% ethanol to remove 2-3 μm of wax. The exposed tissue was then washed, and stained

with Toluidine Blue (0.12% in 1% borax) for 20s [5]. Four overlapping images were acquired using the digital camera and 65 mm macro lens at $1\times$ zoom giving a pixel resolution of $8.33\ \mu\text{m}$. 129 such image planes were acquired over 6.4 mm at $50\ \mu\text{m}$ spacing.

4) *Cochlea*: A cochlea was dissected from a rat ear, embedded in resin and mounted on the stage. Etching for 20s exposed approximately $1\ \mu\text{m}$ of tissue, and Toluidine blue was again used as the tissue stain. The digital camera was mounted on the microscope, and the sample imaged through a $20\times/0.7$ NA glycerol-immersion lens resulting in a pixel resolution of $0.32\ \mu\text{m}$. A grid of 2×5 images were acquired on each image plane, and 410 such planes were acquired over 1.2 mm at mill steps of $3\ \mu\text{m}$.

C. Image Processing

All tissue images were post-processed to maximize image quality, and a 3D image volume was reconstructed.

1) *Cardiac ventricle*: Images were background-corrected against a reference image, and denoised using a Debauchies wavelet-based algorithm. Cross-correlation techniques were used to determine the precise image overlaps, and a montage image was created of each image plane by averaging overlapping regions of the 6×6 grid of images. The final image volume was reconstructed from these montage planes.

2) *Brain cortex*: Images were denoised using a Debauchies wavelet-based algorithm and 3D deconvolution was employed to enhance the images, using an iterative Weiner technique with a theoretical point spread function (PSF). The image volume was reconstructed using the same averaging techniques described above.

3) *Cardiac atria*: Each image was color-corrected using a white balance filter, and montage planes were reconstructed by averaging overlapping pixels. These images were resampled at one-sixth resolution so that the reconstructed volume had an isotropic voxel resolution of $50\ \mu\text{m}$.

4) *Cochlea*: Each image was color-corrected using a white-balance filter and background-corrected against a reference white image. Each image plane was reconstructed from the 10 images by averaging overlapping pixels.

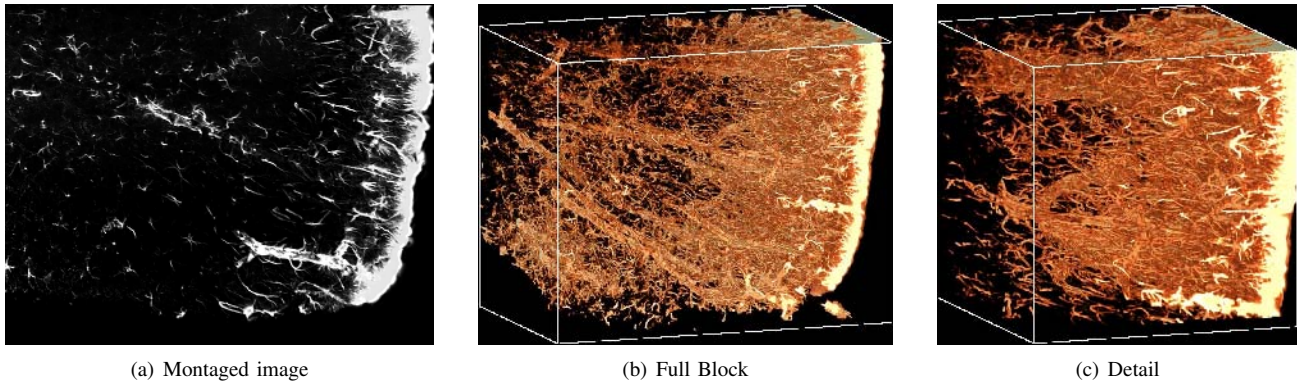


Fig. 3. Brain cortex stained for GFAP. (a) A single image ($500\ \mu\text{m} \times 400\ \mu\text{m}$) montaged from 3×3 overlapping images, following denoising and deconvolution. (b) The full block dimensions are $500\ \mu\text{m} \times 400\ \mu\text{m} \times 300\ \mu\text{m}$. (c) The enlarged region is $250\ \mu\text{m} \times 250\ \mu\text{m} \times 250\ \mu\text{m}$, and shows that the astrocytes are clustered around blood vessels.

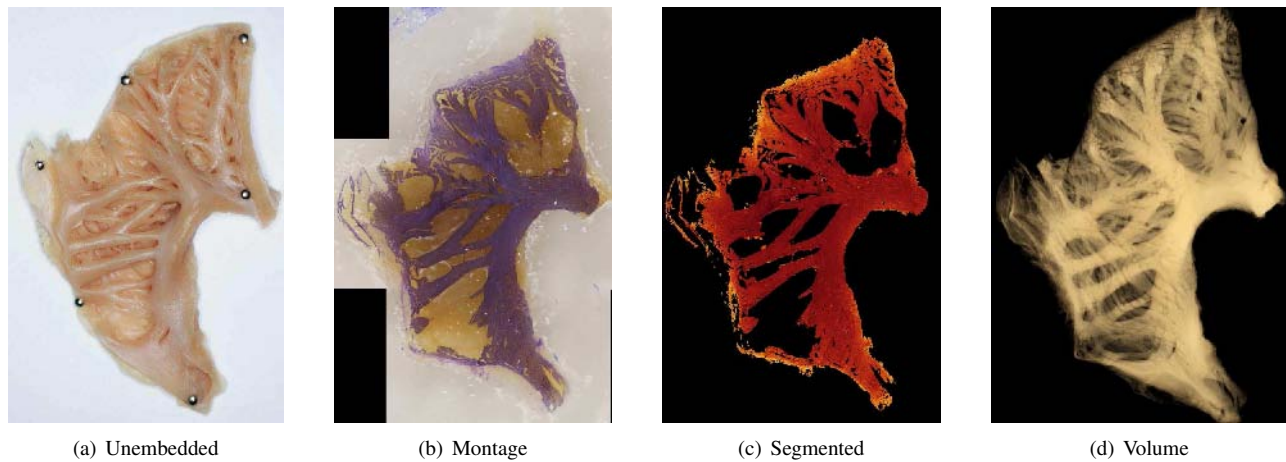


Fig. 4. Cardiac atria stained with Toluidine blue. (a) The atrial appendage before embedding. (b) A montage of 4 images in one image plane. (c) Segmentation of the images according to intensity. (d) The segmented volume is drawn with transparency. The full block dimensions are $54\ \text{mm} \times 36\ \text{mm} \times 6\ \text{mm}$.

III. RESULTS

A. Cardiac ventricle

A sub-volume of $500 \times 500 \times 500$ voxels was cropped from the total image volume, and is visualized in Fig. 2(a). The stained collagen is white, and tissue (which is autofluorescent) is red. The laminar organization of ventricular myocardium is evident as is the network of perimysial collagen that encompasses and interconnects layers. By extracting smaller regions, as in Fig. 2(b), we can see features of the collagen network in greater detail.

B. Brain cortex

A processed image montage, in which the astrocytes are clearly labeled, is presented in Fig. 3(a). The full image volume is rendered in Fig. 3(b), showing the cortical wall and the outline of blood vessels. Detail of the individual astrocytes is apparent in the sub volume in Fig. 3(c).

C. Cardiac atria

An unembedded section of right atrial appendage is shown in Fig. 4(a). The complex structural arrangement of the

pectinate muscles on its endocardial surface is evident. Four overlapping images from one image plane have been processed and composited into a montage in Fig. 4(b). There is a clear color contrast between surface stained tissue, underlying tissue and the surrounding wax. The tissue region was segmented on the basis of color but intensity information was preserved (see Fig. 4(c)). These images were used to reconstruct the rendered volume in Fig. 4(d) where the thin outer wall (where intensity is lower) has been made more transparent. This highlights both the branching structure of the pectinate muscles, and the fiber orientations present within the thin wall.

D. Cochlea

Fig. 5(a) is a slice ($1.8\ \text{mm} \times 2.7\ \text{mm}$) assembled from a montage of 2×5 images with a pixel resolution of $0.32\ \mu\text{m}$. The volume was imaged by acquiring 420 such planes. A sub volume of $656\ \mu\text{m} \times 1088\ \mu\text{m} \times 150\ \mu\text{m}$ was extracted from the region indicated in Fig. 5(b). 15 tissue structures were identified in each of the 50 slices comprising this sub volume using a combination of automated thresholding,

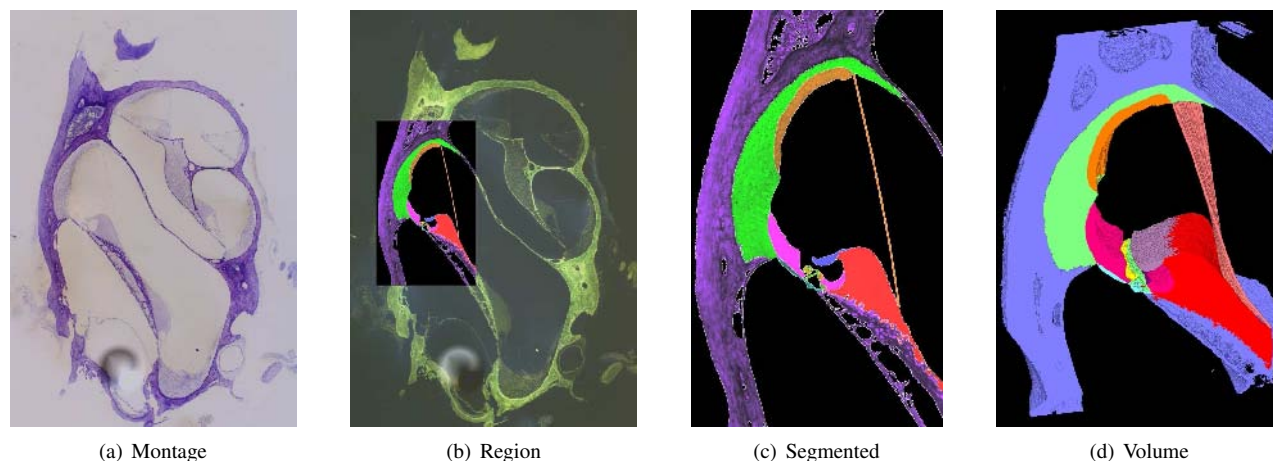


Fig. 5. Rat cochlea stained with Toluidine blue. (a) A single image plane montage of 2x5 images. (b) A small region ($656 \mu\text{m} \times 1088 \mu\text{m}$) was selected from 50 of the image planes for segmenting. (c) Various structures were segmented using a combination of automated and manual techniques. (d) The segmented images are stacked, and viewed in 3D ($0.7 \text{ mm} \times 1.1 \text{ mm} \times 0.15 \text{ mm}$).

edge detection, and manual outlining. A typical segmented image is presented in Fig. 5(c). The 3D arrangement of these structures within the cochlea is shown in the rendered stack presented in Fig. 5(d).

IV. DISCUSSION

The image sets presented here provide detailed information about the 3D organization of tissue structure within volumes much greater than those generally acquired using light or confocal microscopy. Pixel and voxel resolutions range from $0.3 \mu\text{m}$ to $50 \mu\text{m}$, and sample dimensions from 1 mm to 50 mm . Several practical considerations constrain the imaging possibilities.

Using the confocal microscope, we can acquire over 100 million voxels per hour, or about 3 mm^3 per day at $1 \mu\text{m}$ voxel resolution. Acquiring 1 cm^3 at the same resolution would take approximately one year, and result in one terabyte of 8-bit image data. Therefore there is a trade-off between image resolution and the volume imaged. The surface-staining approach is largely constrained by the time required to mill, etch and stain the surface for each image plane, with a typical cycle requiring 3 to 5 minutes.

The use of an ultramill requires the use of embedding materials compatible with the milling process. Confocal microscopy, in particular, works best with resin-embedded specimens since the ultramill produces an optically flat surface under these circumstances. The tissue processing required for wax and resin embedding precludes the use of some immunohistochemical stains. Moreover, when imaging large volumes, perfusion staining is most appropriate, since the penetration that can be achieved with diffusion staining is constrained. This also may be infeasible with some immunohistochemical stains. More flexibility is possible with the surface-staining technique, although the serial nature of the process means that extreme care must be taken (both in staining and in lighting) to ensure consistency in the resulting images, and imaging time can be increased because of the

steps required to mill and stain each image plane.

The confocal images benefit greatly from denoising and deconvolution to reduce the effects of the microscope PSF. These are, however, computationally expensive processes, with the time required for post-processing approximately equal to the image acquisition time. Along with disk storage and archiving requirements, this presents a requirement for efficient image processing and management.

V. CONCLUSIONS

We have constructed an imaging rig capable of acquiring extended volume 3D images at a range of micron and millimeter scales, while maintaining registration and alignment. This enhances previous abilities to image tissue, and is a promising development for large-scale analysis of tissue structure.

ACKNOWLEDGMENTS

We would especially like to thank Adele Pope for the collagen highlighting in Fig. 2(b), Hilary Holloway and Colin Green for their work on the brain cortex, Ram Ganesalingham for the atria, and Dairne Dreaver and Peter Thorne for the cochlea, all at The University of Auckland.

REFERENCES

- [1] G. B. Sands, D. A. Gerneke, D. A. Hooks, C. R. Green, B. H. Smaill, and I. J. Le Grice, "Automated imaging of extended tissue volumes using confocal microscopy," *Microsc. Res. Techniq.*, vol. 67, no. 5, pp. 227–239, 2005.
- [2] J. L. Clendenon, C. L. Phillips, R. M. Sandoval, S. Fang, and K. W. Dunn, "Voxx: a PC-based, near real-time volume rendering system for biological microscopy," *Am. J. Physiol. Cell. Physiol.*, vol. 282, no. 1, pp. C213–218, 2002.
- [3] A. A. Young, I. J. Le Grice, M. A. Young, and B. H. Smaill, "Extended confocal microscopy of myocardial laminae and collagen network," *J. Microsc.*, vol. 192, no. 2, pp. 139–150, 1998.
- [4] H. Holloway, D. A. Gerneke, C. R. Green, I. J. Le Grice, and G. B. Sands, "Resin embedding of immunofluorescently labelled tissue," in *ACMM 18*, Geelong, Australia, 2004.
- [5] D. A. Gerneke, G. B. Sands, R. Ganesalingham, P. Joshi, B. Caldwell, B. H. Smaill, and I. J. Le Grice, "Surface imaging microscopy using an ultramiller for large volume 3D reconstruction of wax- and resin-embedded tissues," in preparation.